arXiv:astro-ph/9708068v1 7 Aug 1997

On The Nature Of The EGRET Source
At The Galactic Center

Sera Markoff[1]*, Fulvio Melia[2]*† and Ina Sarcevic*

*Physics Department, The University of Arizona, Tucson, AZ 85721

†Steward Observatory, The University of Arizona, Tucson, AZ 85721

ABSTRACT

The recent detection of a γ-ray flux from the direction of the Galactic center by EGRET on the Compton GRO raises the question of whether this is a point source (possibly coincident with the massive black hole candidate Sgr A*) or a diffuse emitter. Using the latest experimental particle physics data and theoretical models, we examine in detail the γ-ray spectrum produced by synchrotron, inverse Compton scattering and mesonic decay resulting from the interaction of relativistic protons with hydrogen accreting onto a point-like object. Such a distribution of high-energy baryons may be expected to form within an accretion shock as the inflowing gas becomes supersonic. This scenario is motivated by hydrodynamic studies of Bondi-Hoyle accretion onto Sgr A*, which indicate that many of its radiative characteristics may ultimately be associated with energy liberated as this plasma descends down into the deep potential well. Earlier attempts at analyzing this process concluded that the EGRET data are inconsistent with a massive point-like object. Here, we demonstrate that a more careful treatment of the physics of p-p scattering suggests that a $\sim 10^6\ M_\odot$ black hole may be contributing to this high-energy emission.

Subject headings: acceleration of particles—black hole physics—Galaxy: center—galaxies: nuclei—gamma rays: theory—radiation mechanisms: non-thermal

---

[1]NSF Graduate Fellow.

[2]Presidential Young Investigator.

1. Introduction

X-ray and γ-ray emission have been detected from the Galactic center (Watson et al. 1981; Skinner et al. 1987; Predehl & Trümper 1994; Churazov et al. 1994). The implications for the radio point source Sgr A* are rather interesting, since the X-ray luminosity is not as large as what is expected based on X-ray observations of smaller black hole candidates. Recently, EGRET on board the Compton GRO has identified a central ($< 1^o$) $\sim$ 30 MeV - 10 GeV continuum source with luminosity $\approx 5 \times 10^{36}$ ergs s^{-1} (Mattox 1996; Mattox et al. 1996; Merck et al. 1996). This EGRET γ-ray source (2EGJ1746-2852), appears to be positioned at $l \approx 0.2^o$, but the exact center of the Galaxy, or even a negative longitude, cannot be ruled out completely. Its spectrum can be fit by a hard power-law of spectral index $\alpha = -1.74 \pm 0.09$ ($S = S_0 E^\alpha$), with a cutoff between $4 - 10$ GeV. At lower energies, the COMPTEL data provide useful upper limits (Strong 1996).

These γ-rays may originate either (1) close to the massive black hole, possibly from relativistic particles accelerated by a shock in the accreting plasma (Mastichiadis & Ozernoy 1994), or (2) in more extended features where relativistic particles are known to be present (Pohl 1997). In the former (see also Mahadevan et al. 1997, who considered a thermal distribution of hot protons), the γ-rays may result from the decay of π's produced via p-p collisions of ambient protons with the shock-accelerated relativistic protons. This study concluded that the presence of a $M_h \sim 10^6 \, M_\odot$ black hole was inconsistent with the EGRET data. However, the earlier calculations suffered from over-simplification and an incomplete treatment of the physics of p-p scattering. For example, although the multiplicity of π production (i.e., the number of π's produced per collision) is a strong function of energy, it was approximated with a constant value of 3 when in fact it can change by orders of magnitude.

In addition, ignoring the role of cascading protons is not a valid approximation when the energy carried away by the leading protons can be over 90% of the incoming proton energy. Here we examine the hypothesis of a black hole origin for the γ-rays employing the most current data for the energy-dependent cross-sections, inelasticity, and π multiplicity, together with a self-consistent treatment of the particle cascade.

2. The Physical Picture

Sgr A* is a nonthermal radio source at the center of the Galaxy (e.g., Menten et al. 1997). The large mass ($\sim 1.8 \times 10^6 M_\odot$; Haller et al. 1996; Eckart & Genzel 1997) enclosed within ~ 0.1 pc indicates that this object may be a massive black hole. The nearby IRS 16 cluster of hot giant stars produces a Galactic center wind with velocity $v_{gw} \approx 500 - 700$ km s^{-1} and mass-loss rate $\dot{M}_{gw} \approx 3 - 4 \times 10^{-3} \, M_\odot$ yr^{-1}. A portion of this wind is captured by Sgr A* and accretes inward. The accretion rate ($\lesssim 10^{22}$ g s^{-1}) resulting from this Bondi-Hoyle process is well below the Eddington value, and so the gas attains a free-fall velocity (Melia 1994; Ruffert & Melia 1994), which eventually becomes supersonic, and a shock forms at $r_{sh} \sim 40 - 120 \, r_g$ (Babul et al. 1989), where $r_g \equiv 2GM_h/c^2$ is the Schwarzschild radius. A fraction of the particles may be accelerated to very high energy by the shock. However, the greater synchrotron and inverse Compton efficiency of the e^-'s compared to that of the p's limits the maximum attainable Lorentz factor of the former by several orders of magnitude compared to the latter, and so the (accelerated) e^- contribution to the radiation field is negligible. The relativistic p's are injected through the shock region with a rate $\dot{\rho}_p(E_p) = \rho_o E_p^{-x}$ cm^{-3} s^{-1} GeV^{-1}. In steady state, this leads to a power-law distribution with index $z \sim 2.0 - 2.4$ (Jones & Ellison 1991). In our case, z is determined in part by the p cooling processes and the particle cascade, and as we shall see, $z \gtrsim x$. The normalization ρ_o is related

to the efficiency η of the shock by

$$\int \rho_o E_p^{-x} E_p \, dE_p = \eta L_{grav} \equiv \frac{\eta G M_h \dot{M}}{r_{sh}} \ . \tag{1}$$

These relativistic particles interact with the ambient particles and the magnetic field B, producing photons via synchrotron, inverse Compton scatterings and the decay of mesons created during p-p collisions. Because the injected p's can be ultrarelativistic, leading order nucleons produced in the scattering events also contribute to the spectrum via multiple collisions in an ensuing cascade. The main products in these collisions are π's, which then decay either to photons ($\pi^0 \to \gamma\gamma$) or leptons ($\pi^\pm \to \mu^\pm \nu_\mu$, with $\mu^\pm \to e^\pm \nu_e \nu_\mu$).

Following Melia (1994), one can see that on average the ambient p number density is

$$n_p = \frac{\dot{N}}{4\pi c r_g^2} \left(\frac{r_g}{r}\right)^{3/2} , \tag{2}$$

where $\dot{N} \approx \dot{M}/m_p$ is the p number accretion rate in terms of the mass m_p. If in addition the magnetic field B is in approximate equipartition with the kinetic energy density, then

$$B^2 = \left(\frac{\dot{M}c}{r_g^2}\right) \left(\frac{r_g}{r}\right)^{5/2} \ . \tag{3}$$

The frequency ν_{max} at which the gas becomes transparent lies in the Rayleigh-Jeans portion of the spectrum. This radiation is assumed to be in thermal equilibrium with the e^-'s.

3. Properties of the Particle Cascade

The relativistic p's undergo a series of interactions including $pN \to pN \, M_\pi \, M_{N\bar{N}}$, where N is either a p or a neutron n, M_π represents the energy-dependent multiplicity of π's, and $M_{N\bar{N}}$ is the multiplicity of nucleon/anti-nucleon pairs (both increasing functions of energy). Since $M_{N\bar{N}}/M_\pi < 10^{-3}$ at low energy and even smaller

at higher energies (Cline 1988), we here ignore the anti-nucleon production events. The charge exchange interaction ($p \to n$) occurs roughly 25% of the time (e.g., Begelman et al. 1990). The other possible interactions are $p\gamma \to p\pi^0\gamma$, $p\gamma \to n\pi^+\gamma$, $p\gamma \to e^+e^-p$ and $pe \to eNM_\pi$.

The high-energy cutoff for the injected p distribution is set by determining the Lorentz factor $\gamma_{p,max}$ above which the combined energy loss rate due to synchrotron emission, inverse Compton scattering and hadronic collisions exceeds the rate of energy gain due to shock acceleration. This transition energy depends on the functional form of the inelasticity and the fraction of power transferred to the π's during the p-p collisions.

Using the M_π measured at several center-of-momentum (CM) energies (Alper et al. 1975; Abe et al. 1988; Albajar et al. 1990), one can determine the π injection rate from the p distribution and the physical characteristics of the ambient medium. The particle cascade continues with the emission of γ-rays and leptonic decays. The e^-'s and e^+'s produced in this fashion constitute an energetic population and one must assess their contribution to the spectrum via synchrotron emission and inverse Compton scattering.

For the conditions in Sgr A*, the p-p collisions dominate over all other π production modes. The relevant energy (E_p) range is bounded below by the π production threshold and above by $\gamma_{p,max}$. Using logarithmic bins, and assuming time independence, we first calculate the steady state p distribution $\rho_p(E_p)$ using the diffusion loss equation

$$\rho_p(E_p) = \left[.892 \int R_{pp}(E_p') \Delta \, dE_p' + \dot{\rho}_p(E_p) \right.$$
$$\left. - \kappa_p E_p^2 \frac{\partial \rho_p}{\partial E_p} \right] / [n_p \sigma_{pp}(E_p)c + 2E_p \kappa_p] \ , \tag{4}$$

where $\Delta \equiv \left[\delta(E_p' - \bar{E}_{p,1}) + \delta(E_p' - \bar{E}_{p,2})\right]$ and $R_{pp}(E_p) = n_p \sigma_{pp}(E_p)c\rho_p(E_p)$ cm^{-3}s^{-1}GeV^{-1} is the rate of p-p collisions at energy E_p, and $\kappa_p =$

3

$(4\sigma_T m_e^2/3c^3 m_p^4)(U_B + U_\gamma)$ is the sum of constants appearing in the power $P_{sync} + P_{Compton} \approx \kappa_p E_p^2$. The first term represents the influx of p's having energy E_p as secondaries in p-p collisions between relativistic p's with energies $\bar{E}_{p,1}$ and $\bar{E}_{p,2}$ and the ambient p's (which are effectively at rest). The relationship between E_p and $\bar{E}_{p,1}$ and $\bar{E}_{p,2}$ is unique, as expressed by the delta-functions, and is determined by special relativity and the inelasticity K_{pp}. We use the assumption that on average the two leading p's created travel either parallel or opposite to the boost to simplify our calculations. In the p-p CM frame, we use $K_{pp} = 1.35\,s^{-0.12}$ for $\sqrt{s} \geq 62$ GeV, and $K_{pp} = 0.5$ for $\sqrt{s} \leq 62$ GeV, where the higher energy slope is from Alner et al. (1986), normalized to match the approximately constant low energy value (Fowler et al. 1984).

The cross section σ_{pp} is taken as a function of energy from the most current published data (Barnett et al. 1996). Unfortunately, the highest energy achieved in modern colliders is orders of magnitude below the values attained in our system. However, the data for $\sqrt{s} \gtrsim 100$ GeV have a log-linear form which makes it possible to extrapolate up to much higher E_p. For the entire range, this is within the Froissart upper bound, which states that at extremely high energy, $\sigma_{pp\,\infty} \propto (\ln s)^2$.

The steady state relativistic p distribution resulting from this procedure can then be used to calculate the synchrotron and inverse Compton scattering spectra, following Rybicki & Lightman (1979), and the rate R_{pp} of p-p collisions. For each of these collisions, a multiplicity M_π of π's is produced, with a ratio of charged to neutral particles of roughly 2:1 (exactly when there are two leading p's, otherwise there will be a surplus π^+ to conserve charge). These have a distribution in transverse (to the beam in experiments, in our case to the direction of the boost back to the lab frame) momentum $dN_\pi/dp_\perp$, which is measured as a function of $\sqrt{s}$ at collider experiments. In order to find the energy of the π's in the CM

frame, we also need the parallel component of the momentum, $p_\parallel$, which we extract from the π distribution as a function of the rapidity, y. In the CM frame, $y = (1/2)\ln[(E_\pi^* + p_\parallel)/(E_\pi^* - p_\parallel)]$, and $y \approx -\ln[\tan(\theta/2)]$ for relativistic energies, where $\cos\theta = p_\parallel/\mid p \mid$. At lower energy ($\sqrt{s} \lesssim 200$ GeV), dN_π/dy is Gaussian in shape, the top of which widens gradually into a plateau with increasing energy. The width and the height of this plateau can be fit to functional forms in $\sqrt{s}$. Details of this process are discussed in an upcoming paper. After binning in $p_\perp$, the end product is a distribution $dN_\pi/dp_\perp dy$ of π's in the CM frame, for each p-p collision at any particular CM energy. Given y and $p_\parallel$, and the fact that $E_\pi^* = (m_\pi^2 + p_\parallel^2 + p_\perp^2)^{1/2}$, the distribution (cm^{-3}s^{-1} per p-p collision at E_p) of π's at energy E_π^* follows from a convolution of $(dN_\pi/dp_\perp dy)dp_\perp dy$ with R_{pp}.

Each of the photons produced in the π^0 decay acquires a rest frame energy $\epsilon_\gamma' = (1/2)m_\pi c^2$ and is emitted with equal probability in any direction. The photon number density in the observer's (or lab) frame must therefore be

$$\rho_\gamma(\epsilon_\gamma)\,d\epsilon_\gamma = \frac{2\,d\epsilon_\gamma}{\beta_\pi \gamma_\pi m_\pi c^2}\,, \qquad (5)$$

where γ_π and β_π are the π Lorentz factor and dimensionless velocity, respectively, in this frame. Finally, the photon emissivity is given by the multiple integral expression

$$j_\gamma(\epsilon_\gamma) = \int \rho_\gamma(\epsilon_\gamma)\frac{dN_\pi}{dp_\perp dy}R_{pp}(E_p)\,dE_p\,dp_\perp\,dy$$
$$\text{photons cm}^3\ \text{s}^{-1}\ \text{MeV}^{-1}\,. \quad (6)$$

The charged π's decay to leptons, which can themselves be a source of radiation from synchrotron and Compton processes. We follow a procedure for the $e^\pm$ completely analogous to that developed above to find the steady state $e^\pm$ distribution:

$$\dot{\rho}_e(E_e) = -2\kappa_e\,E_e\,\rho_e(E_e) - \kappa_e\,E_e^2\,\frac{\partial\rho_e(E_e)}{\partial E_e}\,. \qquad (7)$$

This equation is easy to solve for the distribution $\rho_e(E_e)$, which we then use to calculate the synchrotron and inverse Compton spectra from the cascade $e^{\pm}$s. Here, $\kappa_e \equiv (4/3)\sigma_T c/(m_e c^2)^2(U_B + U_\gamma)$.

4. Results and Discussion

When the shock is located at $r_{sh} = 40r_g$, we have $B \approx 435$ Gauss and $n_p \approx 1.6 \times 10^9$ cm^{-3}. The Rayleigh-Jeans tail cuts off at $\nu_{max} \approx 10^{13}$ Hz, with a temperature $\approx 6.3 \times 10^9$ K. Thus, $\gamma_{p,max} \approx 1.2 \times 10^9$. We find that for the environment of Sgr A*, unlike those of typical AGNs, the p-p collisions dominate over p-γ by at least ten orders of magnitude over the entire energy range. This is because of the relatively low density of ambient baryons, and the extreme dearth of photons due to the low value of ν_{max}. Because of this, we neglect the contribution from all p-γ interactions. We can similarly neglect p-e collisions for this system, the cross-section of which is $\approx \frac{1}{137}\sigma_{pp}$. Since the population of relativistic e^-'s is much smaller than that of ambient p's, the contribution is insignificant. The synchrotron cooling channel dominates at the highest energy, and is the other significant contributor to the spectrum. From Sikora et al. (1989), we find that any relativistic n's with Lorentz factor $\gamma_n \lesssim 10^8$ will escape the system without interacting, so we consider as lost any n's produced in the cascade. The low photon density also means the region is extremely optically thin to high-energy photons, so we consider the spectrum observed at Earth to be that produced at the shock. By comparison, $\gamma_{e,max} \approx 6.5 \times 10^5$ for the e^-'s, corresponding to an energy of 3.3×10^5 MeV. For a roughly equal injection rate of relativistic e^-'s and p's, this energy content is significantly below that of the cascade e^-'s, which therefore dominate the leptonic contribution to the photon spectrum.

In all, five spectral components may be contributing to 2EGJ1746-2852: p synchrotron, p inverse Compton scattering, $e^{\pm}$ synchrotron, $e^{\pm}$ inverse Compton scattering, and π^0 decay. For a reasonable efficiency (i.e., $\eta \lesssim 10\%$), the p synchrotron spectrum dominates over that of the photons from π^0 decay as long as the p injection index $x \lesssim 2.2$. In Figure 1, we show these components for the case when $r_{sh} = 40r_g$, and $x = 2.0$ with an efficiency of 1%. The p synchrotron seems to fit the data reasonably well, but clearly misses the apparent low energy turnover in the EGRET data, and the upper limits for the highest energy COMPTEL points. This could be due to the simplified geometry we have adopted in this paper, but this is unlikely since the synchrotron spectrum depends primarily on the particle physics. It is also evident in Figure 1 that Compton scattering is not important for this source, and that the cascade $e^{\pm}$'s are relatively ineffective. The photons produced by π decay are also insignificant. Placing the shock at $120r_g$ instead of $40r_g$ (Fig. 2) increases the emission area while decreasing B, and the p synchrotron spectrum misses more data at the low end of the EGRET spectrum. The $e^{\pm}$ components still do not contribute.

With the shock at $40r_g$, the π^0 decay spectral component begins to dominate over synchrotron when $x \gtrsim 2.2$. In Figure 3, we show the same five components for the case $x = 2.4$, which leads to $z = 2.46$. Here, $\eta \approx 9\%$. The shape of the π^0-induced γ-ray spectrum can be understood as follows. The center of the curve is set by the energy ($\epsilon_\gamma = 67.5$ MeV) of the decay photons in the π^0 rest frame, and the width is determined by Doppler broadening. The slope of the sides, and hence the index of the EGRET spectrum, is due to the falloff in the number of decaying π's at higher energy. Each π decay produces a flat photon spectrum (see Eq. 5) whose width increases with E_π. So the cumulative effect of all the decays is greatest near $\epsilon_\gamma = 67.5$ MeV, where all π's contribute. The relative contribution to the spectrum at lower or higher ϵ_γ then depends on the overall π distribution, which in turn is a function of both M_π and $\rho_p(E_p)$. The flattened top, and hence the low-energy turnover

in the π decay spectrum, is due to the cutoff in π production near the threshold. The π decay spectrum cannot be translated laterally, so a simultaneous match of both this turnover and the spectral slope is significant.
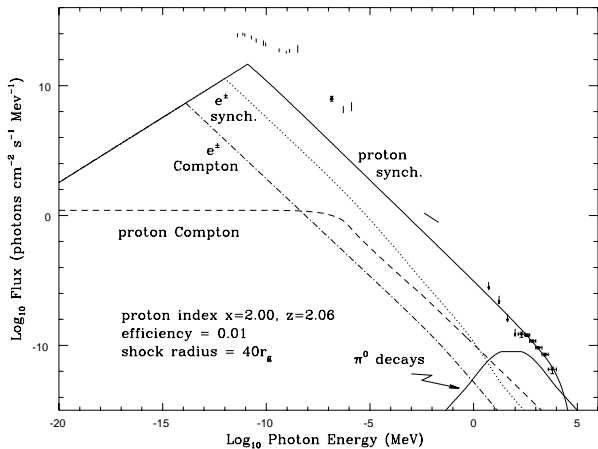

Fig. 1.— Five spectral components (as labeled) resulting from the p-p cascade. The shock is here located at $40r_g$, and the injected proton spectral index is $x = 2.00$, yielding a steady state proton index $z = 2.06$. The inferred efficiency in this case is $\eta = 1\%$. The data points are from: (radio) Lo (1987), Zylka et al. (1993); (IR) Eckart et al. (1993), Stolovy (1996); (X-rays) Pavlinskii et al. (1992); (γ-rays) Strong 1996, Mattox (1996).

The required efficiency for producing the EGRET spectrum is different depending on whether synchrotron or π decay emissivity dominates. There are three exit channels for the processed p energy: (i) p synchrotron, (ii) $\pi^0 \to \gamma\gamma$, and (iii) $\pi^\pm \to \mu^\pm \nu_\mu$, with $\mu^\pm \to e^\pm \nu_e \nu_\mu$. The latter two are coupled by a fixed ratio since each of the three types of π's receives an equal fraction of the energy lost by the colliding p's. When $x \lesssim 2.2$, (i) dominates and the conversion of p power to photons is very efficient. When $x \gtrsim 2.2$, (ii) & (iii) dominate, but the fraction of p power going into photons rather than particle by-products is now smaller, so a higher η is needed.
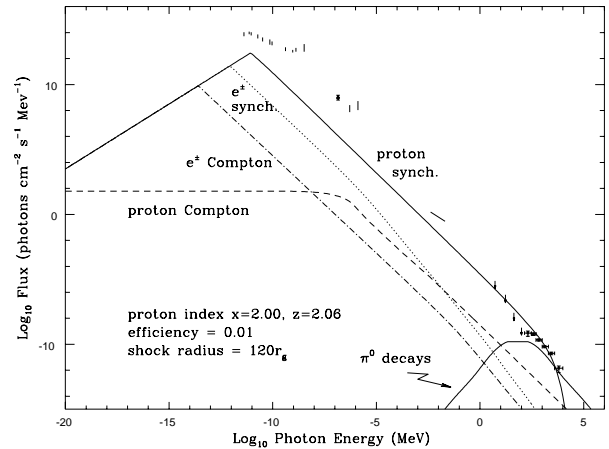

Fig. 2.— Same as Fig. 1, except for a shock located at $120r_g$.

A population of relativistic p's energized within an accretion shock near a super-massive black hole at the Galactic center may be contributing to the ~ 30 MeV–10 GeV emission from this region. Depending on the value of the injected p index (i.e., $x \lesssim 2.2$ or $x \gtrsim 2.2$), this contribution may come either from synchrotron or π^0 decay. However, the synchrotron emissivity cannot account for the turnover in the EGRET spectrum and some of the COMPTEL upper limits at $\epsilon_\gamma \sim 100$ MeV, whereas the π-induced photon distribution has a natural flattening there due to the threshold for π production in p-p scatterings. We have not yet undertaken a detailed χ^2 fitting to find the optimal parameters. However, it may be an indication of robustness in the model that a good fit was obtained without any fine-tuning. A more sophisticated fitting using the actual data will be undertaken in the future. Our methods and results differ significantly from earlier treatments. Our use of M_π and a careful treatment of the particle cascade give a good fit to the γ-ray spectrum with reasonable parameters, such as $z \approx 2.5$, $\eta \approx 0.09$, and a black hole mass $M_h \sim 10^6 \, M_\odot$ (cf. Mastichiadis & Ozernoy 1994 who concluded that $z \approx 1.7$, and $M_h \ll 10^6 \, M_\odot$).
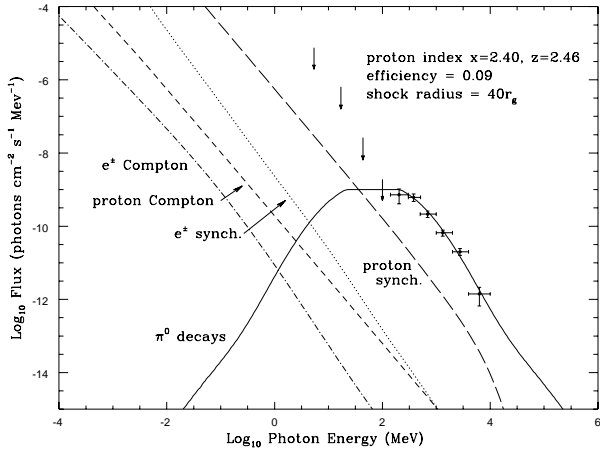
Fig. 3.— Same as Fig. 1, except that the spectrum is here magnified to highlight the EGRET and COMPTEL energy range. In addition, the proton injection index is $x = 2.4$, yielding a steady state proton index $z = 2.46$. The inferred efficiency is here $\eta = 9\%$.

5. Acknowledgments

REFERENCES

Abe, F. et al. 1988, *PRL*, **61**, 1819.

Albajar, C. et al. 1990, *Nuc. Phys. B*, **335**, 261.

Alner, G. et al. 1986. *Zeits.Phys.*, **33C**, 1.

Alper, B. et al. 1975, *Nuc. Phys. B*, **100**, 237.

Babul, A., Ostriker, J. & Mészáros, P. 1989, *ApJ*, **347**, 59.

Barnett, R. et al. 1996, *Phys.Rev.*, **D54**, 1.

Begelman, M., Rudak, B. & Sikora, M. 1990, *ApJ*, **362**, 38.

Churazov, E., et al. 1994, ApJS, 92, 381.

Cline, D. 1988, Proceedings of the RAND Workshop on Antiproton Science and Technology, Ed. B.W. Augenstein, et al. (New Jersey: World Scientific), 45.

Eckart, A. et al. 1993, *ApJ (Letters)*, **407**, L77.

Eckart, A. & Genzel, R. 1997, *MNRAS*, **284**, 576.

Fowler, G. et al. 1984, *Phys.Lett.*, **145B**, 407.

Haller, J. et al. 1996, *ApJ*, **468**, 955.

Jones, F. & Ellison, D. 1991, *SSRv*, **58**, 259.

Lo, K.Y. 1987, in AIP Proc. 155, ed. D.C. Backer (AIP: New York), **155**, 30.

Mahadevan, R., Narayan, R. & Krolik, J. 1997, astro-ph , 9704018.

Mastichiadis, A. & Ozernoy, L. 1994, *ApJ*, **426**, 599.

Mattox, J.R. 1996, *GCNEWS* *http://www.astro.umd.edu∼gcnews/gcnews/Vol.4/article.h* **4**.

Mattox, J.R. et al. 1996, *ApJ*, **461**, 396.

Melia, F. 1994, *ApJ*, **426**, 577.

Menten, K., Reid, M., Eckart, A. & Genzel, R. 1997, *ApJ (Letters)*, **475**, L111.

Merck, M. et al. 1996, A&AS, 120, 465.

Pavlinskii, M., et al. 1992, Soviet Astr. Lett., 18, 291P.

Pohl, M. 1997, A&A, 317, 441.

Predehl, P. & Trümper, J. 1994, A&A, 290, L29.

Ruffert, M. & Melia, F. 1994, A&A, 288, L29.

Rybicki, G. & Lightman, A. 1979, Radiative Processes in Astrophysics, (New York: Wiley), 179 & 207.

Sikora, M. Begelman, M. & Rudak, B. 1989, *ApJ (Letters)*, **341**, L33.

Skinner, G.K., Willmore, A.P., Eyles, C.J., Bertram, D. & Church, M.J. 1987, *Nature*, **330**, 544.

Stolovy, S.R., Hayward, T.L. & Herter, T. 1996, *ApJ (Letters)*, **470**, L45.

Strong, A. W. 1996, private communication to Pohl, M..

Watson, M.G., Willingale, R., Grindlay, J.E., & Hertz, P. 1981, *ApJ*, **250**, 142.

Zylka, R., Mezger, P.G. & Lesch, H. 1993, A&A, 261, 119.